IEEE Access
Multidisciplinary | Rapid Review | Open Access Journal

Received December 11, 2018, accepted December 22, 2018, date of publication December 28, 2018,
date of current version January 23, 2019.

Digital Object Identifier 10.1109/ACCESS.2018.2890157

Numerical Analysis of Thermo-Electric Field for AC XLPE Cable in DC Operation Based on Conduction Current Measurement

XIANGRONG CHEN, (Member, IEEE), JINGZHE YU, (Student Member, IEEE), LINWEI YU, AND HAO ZHOU

Zhejiang Provincial Key Laboratory of Electrical Machine Systems, College of Electrical Engineering, Zhejiang University, Hangzhou 310027, China

Corresponding author: Xiangrong Chen (chenxiangrongxh@zju.edu.cn)

This work was supported in part by the National Key R&D Program of China under Grant 2018YFB0904400, in part by the Natural Science Foundation of Zhejiang Province under Grant LY18E070003, in part by the Fundamental Research Funds for the Central Universities under Grant 2018QNA4017, and in part by the One-hundred Talents Program of Zhejiang University (A).

ABSTRACT With rapid development of renewable energies and dc loads in distribution grids, converting ac distribution grids into dc operation has become a promising method to utmost utilize the present ac distribution grid in large cities. This paper reports a numerical investigation of thermo-electric fields of a three-core 10-kV ac cross-linked polyethylene (XLPE) cable and cable joint in the dc operation. DC conduction current for the XLPE and silicon rubber (SiR) was evaluated at different temperatures and electric fields. The thermo-electric field simulation was performed by COMSOL Multiphysics according to the measured data. The obtained result showed that the threshold of XLPE at 65 °C is 3.1 MV/m, whereas the threshold of SiR at 60 °C is 2.2 MV/m. It was found that the maximum electric field of the cable operated in dc voltage up to 12.5 kV was below the threshold of 3.1 MV/m. The maximum electric field in the cable joint appeared at the high voltage screen tube, whereas the maximum electric field at the high voltage screen tube was less than the threshold of SiR at a temperature difference of 25 °C. Moreover, the maximum transmission power of the three-core 10-kV AC XLPE cables running at the ±10-kV bipolar dc operation was 1.36 times of the power in the ac operation. It was elucidated that the three-core ac 10-kV XLPE cable could be operated reliably at ±10 kV in bipolar dc topology with sufficient safety margin. It is beneficial to upgrade the ac distribution grid to the dc distribution grid.

INDEX TERMS XLPE cable, cable joint, bipolar DC operation, conduction current, space charge, thermo-electric field.

I. INTRODUCTION

Nowadays traditional alternating current (AC) distribution grids are facing many challenges caused by booming renewable energies and direct current (DC) loads. AC/DC converters, energy storage devices and complex control systems are required to integrate the renewable energies and DC loads in the present AC grids. However, the integration of the renewable energies and DC loads are relatively simple in DC distribution grids. The DC distribution grid also has advantages in terms of power transmission capacity, controllability and power quality. It has been received more and more attentions around the world [1]–[6]. Furthermore, new DC distribution grids in mega-cities are difficult to build due to a shortage of land resources and a saturation of underground spaces. A direct method to solve the limited space challenges is to operate the present AC distribution grid at DC voltage. It will utmost use the AC grids and save construction costs to build the new DC distribution grids. Cross-linked polyethylene (XLPE) insulated cables are widely used for the medium-voltage (MV) AC distribution grid in the cities. In order to transfer the AC distribution grid into the DC distribution grid, it is indispensable to investigate a feasibility of converting the AC XLPE cables for DC applications.

Liu et al reported a scheme of upgrading an existing 35 kV AC XLPE cable into ±10 kV bipolar DC operation for the first time in China [7]. The AC distribution line was changed into bipolar DC line. Two phases of the three-phase cables were used as the positive and negative lines, whereas the third phase cable was used as ground. An innovative ANGLE DC project will convert two existing 33 kV AC distribution

circuits from the island of Anglesey to the Welsh mainland to operate as ±27 kV bipolar DC circuits in the UK [8].

For the AC XLPE cable operated at bipolar DC voltages, the space charge would accumulate in the XLPE cable insulation and the insulation of cable accessories. The accumulated space charge in the insulation can increase the rate of degradation through local field enhancement, ionization/excitation and electromechanical energy storage, leading to considerable endurance (accelerated ageing) problems for the cable [9]. However, there is an electric field threshold that the space charge begins to accumulate rapidly for the polymeric insulating materials [10]. When the electric field is below the threshold value, the amount of space charge accumulation is insignificant. The cable designed close to the threshold would significantly reduce problems of accelerated degradation caused by the presence of space charge [9]. In order to guarantee a safe and reliable long service of the cables in DC operation, it is essential to limit the electric field in the cable below the threshold value.

In this paper, the threshold of the space charge accumulation and DC conductivity of the cable insulating materials were evaluated by conduction current measurements. Based on the measured data, a three-core 10 kV AC XLPE cable and its cable joint were used to perform the thermo-electric coupling simulations by finite element analysis software COMSOL Multiphysics. The thermo-electric coupling field of the cable in bipolar DC operation was evaluated at different temperature differences and DC voltages. The feasibility and benefits of converting the 10 kV AC cable into ±10 kV DC application was proposed.

II. EXPERIMENTAL AND SIMULATION MODEL

There are basically two methods to evaluate the electric field threshold of the space charge accumulation in the insulating materials. One method is to directly measure the accumulated space charge in the materials at different electric fields and temperatures. It has been shown that the field threshold of space charge accumulation corresponds to the electric field at which the inflection of the conduction current characteristic occurs [11]–[16]. Thus the other method is to measure the current density of the materials at different electric fields.

Fabiani et al reported that the electric field threshold of XLPE is 8 MV/m at 25 °C, whereas the electric field threshold is 3 MV/m at 70 °C [17]. Vu et al showed that the threshold of XLPE is 10 MV/m at 20 °C, and the threshold is less than 2 MV/m at 70 °C [18]. Considering the real operation environment of the cable, the electric field threshold of XLPE and Silicon rubber (SiR) used for 10 kV AC XLPE cable was evaluated at different temperatures and electric fields.

A. SAMPLE PREPARATION

XLPE material used for 10 kV AC cable was provided by Nanjing Zhongchao New Materials Corporation in China. Disk-like films with a diameter of 90 mm and a thickness of ∼200 μm were prepared by a heating press method. The procedure was performed at 180 °C, initially for 3 minutes at a pressure of 2 kN and the following 15 minutes at a pressure of 200 kN. With the pressure on, the film was cooled down to room temperature at an approximate rate of 5 °C/min. After the manufacture, all the films were degassed (<102 Pa) in a vacuum chamber at 80 °C for two days.

SiR used for AC 10 kV cable joint was supplied by Changlan Electric Technology Corporation in China. Specimen with a diameter of 90 mm and a thickness of ∼200 μm were prepared by the heating press method mentioned above. The process was carried out at 120 °C for 15 minutes at a pressure of 150 kN. With the pressure on, the sample was cooled down to room temperature at an approximate rate of 5 °C/min. The samples were degassed (<102 Pa) in a vacuum chamber at 80 °C for two days.

B. DC CONDUCTION CURRENT MEASUREMENT

The DC conduction current measurement setup is shown in Fig. 1. It includes of a high voltage DC supply (Glassman FJ60R2, 60 kV, 2 mA, USA), a three-electrode system, Keithley electrometer 6517B (Keithley Instruments, Solon, OH, USA). The high voltage electrode is a stainless steel cylinder with a diameter of 45 mm. The measuring electrode was 30 mm in diameter, whereas the guard ring with diameter of 45 mm allowed for eliminating surface leakage current. The electrode system and film sample was put in a thermal chamber.

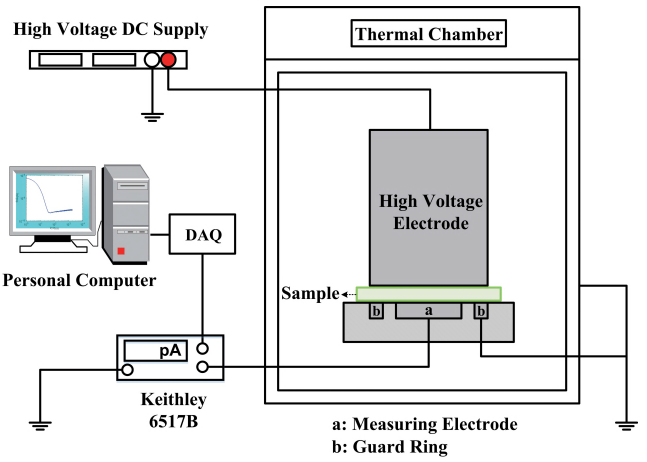

FIGURE 1. The DC conduction current measurement setup.

The conduction current of the XLPE was recorded for 30 min at 2-20 MV/m with controlled temperatures of 30, 40, 50, 60, 65 and 70 °C, respectively. The conduction current of the SiR was recorded for 30 min under 1-20 MV/m with controlled temperatures of 30, 40, 50, 60 and 70 °C, respectively. The electric field threshold and DC conductivity were estimated by the measured conduction current.

C. THE STRUCTURE PARAMETERS OF CABLE

A three-core 10 kV AC XLPE cable was used in the cable simulation. Fig. 2 shows the simplified two-dimensional cable simulation model for the cable operated at DC voltages.

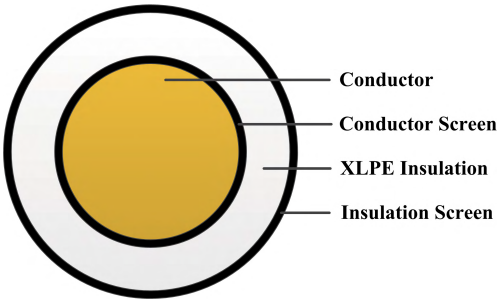

FIGURE 2. The simplified structure for cable simulation.

The conductor (Cu) radius of the cable is 9.15 mm and the XLPE insulation thickness is 4.5 mm. The thickness of the conductor and insulation screen is 0.8 mm.

D. THE STRUCTURE AND PARAMETERS OF CABLE JOINT

A cable joint of the 10 kV AC XLPE cable was used in the cable joint simulation. Fig. 3(a) shows a two-dimensional structure of the cable joint. Fig. 3(b) demonstrates a three-dimensional model that was obtained through a 360° rotation of the two-dimensional structure utilizing the horizontal symmetry line as a rotating axis. The three-dimensional model of the cable joint was used for the simulations.

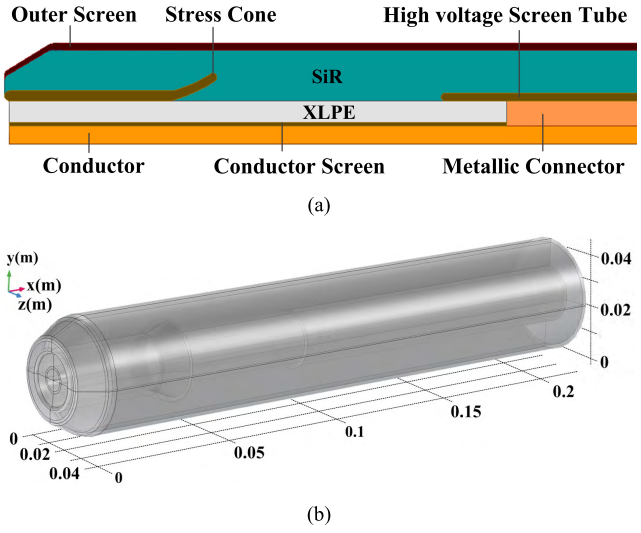

FIGURE 3. The two-dimensional structure (a) and three-dimensional model (b) of the cable joint.

According to the data provided by the cable joint supplier, the conductivity of the semi-conductive material used for the conductor screen, insulation screen, outer screen, stress cone and high voltage screen tube is 5×10^{-2} S/m. And the thermo-physical parameters of the materials for the cable and cable joint are listed in Table 1.

E. BASIC EQUATIONS

In the case of thermal field simulations, the thermal conductivity of the materials remains constant in the temperature range of the cable operation. The stationary heat conduction equation [19] can be expressed as:

$$\lambda\nabla^2 T + \phi = 0 \tag{1}$$

where λ is the thermal conductivity, T is the temperature, ϕ is the heat source intensity. The temperature of copper conductor was set as a constant value as the heat source in the thermal simulations, whereas the temperatures of the outermost layer of the cable and cable joint were also set as constant values in the simulation. Furthermore, boundaries of outermost layer were set to be thermal insulated, and without convective boundary conditions.

For electric field simulations, the voltage was applied on the conductor. The screen was grounded. The equation of electric potential [19] is given by:

$$\nabla(\gamma \cdot \nabla U) + \varepsilon_0\varepsilon_r\frac{\partial(\nabla U)}{\partial t} = 0 \tag{2}$$

where γ is the conductivity of the insulation materials, U is the electric potential, ε_0 is the vacuum permittivity, ε_r is the relative permittivity of the insulation materials, and t is the time. The simulation was performed without a consideration of the accumulated space charge in the insulation as the electric field was near or below the threshold value. Moreover, the measured conductivities of the XLPE and SiR were used in the thermo-electric simulations due to the temperature and electric field related DC conductivity of the materials.

TABLE 1. The thermo-physical parameters of the materials in the cable and cable joint.

Materials	Density ($kg\cdot m^{-3}$)	Specific heat ($J\cdot kg^{-1}\cdot K^{-1}$)	Thermal conductivity ($W\cdot m^{-1}\cdot K^{-1}$)
Copper	8900	380	385
XLPE	1200	1000	0.286
SiR	1150	1300	0.27
Semi-conductive	1200	1100	0.28

III. EXPERIMENTAL RESULTS AND DISCUSSION

A. CONDUCTION CURRENT DENSITY

The conduction current density vs. electric field (J-E) of the XLPE measured at different temperatures is shown in Fig. 4. The regression lines to the data at low and high fields are also illustrated in the figure. The result shows that two slopes are presented for the XLPE at the temperature from 30 °C up to 65 °C with an increase of the electric field, but only one slope could be obtained at 70 °C. According to the definition of the threshold for the space charge accumulation in the insulation materials [11], the intersection of the fitted lines were found as the threshold of XLPE. It is seen that the threshold of the XLPE is decreased consistently with the increased of the temperature.

Fig. 5 shows the conduction current density vs. electric field of the SiR at different temperatures. Similarly to the XLPE, there are two conduction regions for the SiR from

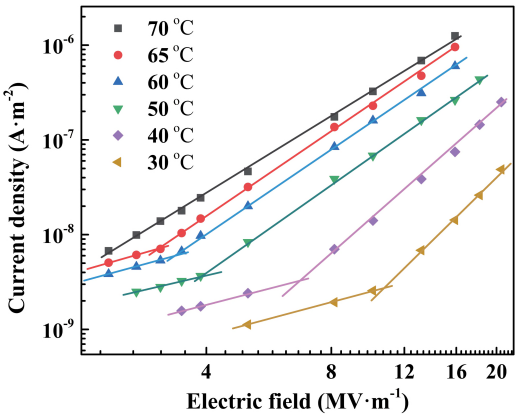

FIGURE 4. Current density vs. electric field of the XLPE in log-log scale at different temperatures.

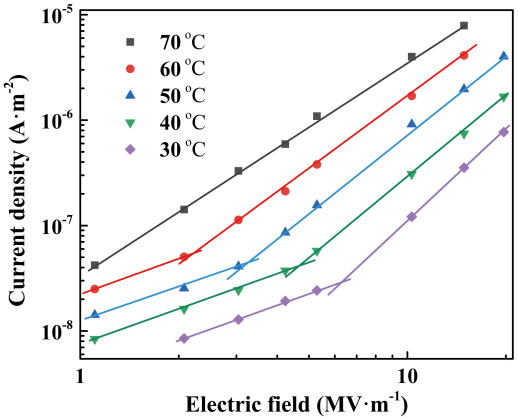

FIGURE 5. Current density vs. electric field of the SiR in log-log scale at different temperatures.

30 °C to 60 °C, and only one conduction region at 70 °C. The threshold of the space charge accumulation for the SiR is also reduced continually with the increase of the temperature.

The electric field thresholds of the space charge accumulation for the XLPE and SiR are summarized in Table 2. The results show that the threshold of the XLPE is higher than the SiR at the measured temperature. Furthermore, it can be seen that the electric field threshold of the space charge accumulation decreases evidently with the increase of the temperature.

TABLE 2. The electric field threshold of the XLPE and SiR at different temperatures.

Threshold field	65 ºC	60 ºC	50 ºC	40 ºC	30 ºC
XLPE (MV·m^{-1})	3.1	3.4	3.8	6.7	10.7
SiR (MV·m^{-1})	-	2.2	3.2	4.6	6.3

Table 3 illustrate a summary of the estimated slope of the conduction region for the XLPE and SiR at different temperatures. The results show that the slopes of the materials are at around 1 below the threshold. It indicates that

TABLE 3. The slopes of the XLPE and SiR at different temperatures.

Threshold field		70 ºC	65 ºC	60 ºC	50 ºC	40 ºC	30 ºC
XLPE	Ohm	-	1.17	1.15	1.07	1.16	1.19
	Non Ohm	2.71	2.91	2.92	3.08	3.87	4.14
SiR	Ohm	-	-	1.12	1.05	1.11	1.12
	Non Ohm	2.01	-	2.26	2.50	2.61	2.85

the current-field relationship obeys Ohm's law in the low field region (Ohm region). However, the slopes are over 2 above the threshold (Non Ohm region), and the slope of both materials decreases gradually with the increase of the temperature. This behavior is usually attributed to the space-charge-limited-current (SCLC) mechanism for polymeric materials [11].

B. DC CONDUCTION

The conduction current data in the Ohm region were used to calculate the DC conductivity of the XLPE and SiR. The DC conductivity γ was estimated by:

$$\gamma = \frac{I}{V}\frac{4h}{\pi d^2} \tag{3}$$

where V is the applied DC voltage, h is the sample thickness, d is the diameter of the measuring electrode, and I is the conduction current.

The formula used to fit the experimental data for DC conductivity calculations in the simulation is expressed as [19]

$$\gamma(E,T) = A\exp[\frac{-\varphi q}{k_b T}]\frac{\sinh(B|E|)}{|E|} \tag{4}$$

where A is a material related constant, φ is the activation energy, q is the electronic charge, k_b is the Boltzmann constant, T is the absolute temperature, B is a dependent coefficient of conductivity on electric field, and E is the electric field.

The experimental and fitted DC conductivity of the XLPE at different temperatures in the Ohm region is illustrated in Fig. 6. The results show that the fitted conductivity is in good agreement with the measured data. Fig. 7 shows the measured and fitted DC conductivity of the SiR at different temperatures in the Ohm region. The results also show that the fitted lines well agree with the experimental data. Moreover, the DC conductivity of the XLPE is lower than the conductivity of the SiR at each temperature. Coefficient obtained for the conductivity fitting of the XLPE and SiR is shown in Table 4. These coefficients were used for the following thermo-electric field simulation of the cable and cable joint in the DC operation.

IV. SIMULATION RESULTS AND DISCUSSION OF CABLE

During the simulation of the cable, the conductor operating temperature was set at 65 °C with the threshold field of 3.1 MV/m (see Table 2). The conductor voltage was DC

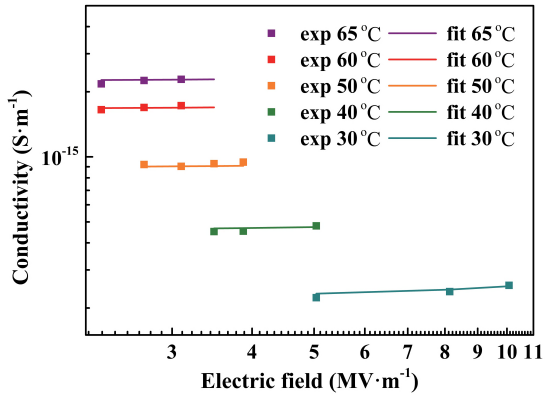

FIGURE 6. The experimental and fitted DC conductivity of the XLPE at different temperatures.

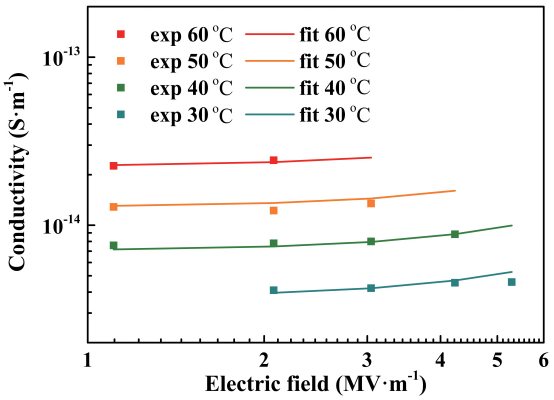

FIGURE 7. The experimental and fitted DC conductivity of the SiR at different temperatures.

TABLE 4. Coefficients for the conductivity fitting of the XLPE and SiR.

Coefficient	A	φ (eV)	B (m·V^{-1})
XLPE	12.2	0.58	8×10^{-8}
SiR	5.8	0.52	2.8×10^{-7}

10 kV. The voltage of the insulating screen was grounded. In order to achieve different temperature difference between the conductor and insulation screen (ΔT_1), the insulation screen temperature was set to be 62.5 °C, 60 °C, 57.5 °C and 55 °C, respectively. Considering the relative thin insulation thickness of the cable, the maximum value of ΔT_1 was set at 10 °C in the simulation.

The obtained steady electric field distributions in the XLPE cable insulation at different ΔT_1 are illustrated in Fig. 8. The results show that the electric field gradually decreases along the radial direction at the ΔT_1 of 2.5 °C and 5 °C, the maximum electric field appears at the inner surface of the insulation. However, the electric field gradually increases along the radial direction at the ΔT_1 of 7.5 °C and 10 °C, the maximum electric field reversely appears at the outer surface of the insulation. The results also indicate that a certain temperature difference is beneficial for balancing the

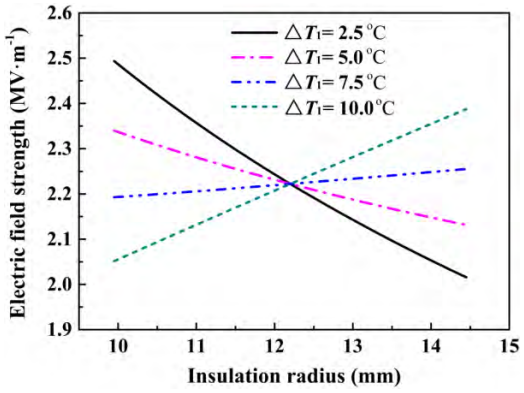

FIGURE 8. The steady electric field distribution in the XLPE cable insulation at different temperature differences.

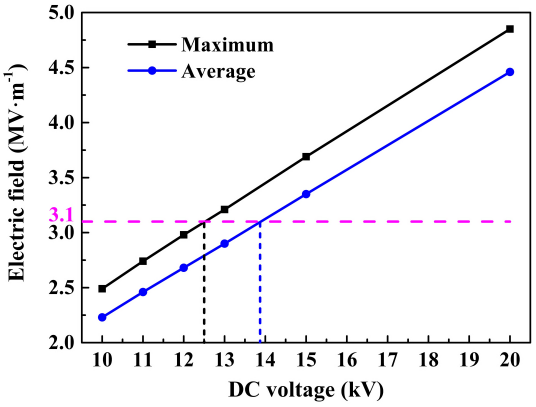

FIGURE 9. The maximum and average electric fields in the XLPE cable insulation at different DC voltages.

electric field distribution on the insulation, e.g. ΔT_1 at 5 °C and 7.5 °C.

It is seen that the highest electric field for the selected ΔT_1 happens at 2.5 °C, whereas the threshold at 65 °C is the lowest at 3.1 MV/m according to the Table 2. In the case of ΔT_1 of 10 °C, the electric field was reversed with the maximum field appeared at the outer surface of the insulation, but the temperature at the outer surface was 55 °C, in which a relative high threshold should be selected. The ΔT_1 at 2.5 °C has a higher possibility of the space charge accumulation comparing to the other temperature differences.

Electric fields in the cable insulation were calculated at different steady DC voltages of the conductor with the ΔT_1 of 2.5 °C. Fig. 9 shows the estimated maximum electric field and the average electric field.

The results in Fig. 9 demonstrate that the maximum electric field of the applied DC voltage up to 12.5 kV is below the threshold of the space charge accumulation of 3.1 MV/m, whereas the average electric field of the DC voltage up to near 14 kV is also below the threshold of 3.1 MV/m. It can be seen that the three-core 10 kV AC XLPE cable can be operated at ±10 kV in bipolar DC topology with sufficient safety margin.

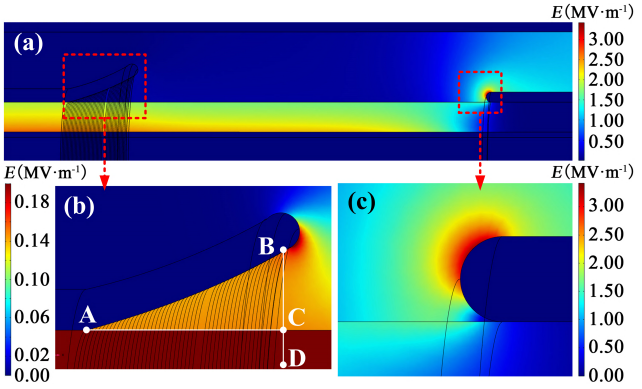

FIGURE 10. The electric field distribution of the cable joint at ΔT_2 of 10 °C. (a) An overview of the electric field distribution. (b) The electric field distribution near the stress cone. (c) The electric field distribution near the high voltage screen tube.

V. SIMULATION RESULTS AND DISCUSSION OF CABLE JOINT

The conductor operating temperature was still set at 65 °C. In order to obtain different temperature difference between the conductor and outer screen (ΔT_2), the outer screen temperature was set to be 55 °C, 50 °C, 45 °C and 40 °C, respectively. The conductor voltage was DC 10 kV. The stress cone and outer screen were grounded.

Fig. 10 shows the electric field distribution of the cable joint at ΔT_2 of 10 °C. The results show that the maximum electric field in the cable joint appeared at the high voltage screen tube. The obtained result was 3.28 MV/m, as shown in Fig. 10(c). The estimated temperature near the high voltage screen tube was at around 59 °C. According to the Table 2, the electric field threshold of the SiR is 2.2 MV/m at 60 °C. It indicates that the space charge would accumulate near the high voltage screen tube. The maximum electric field near the stress cone was at around 0.18 MV/m in the SiR insulation as illustrated in Fig. 10(b). Table 5 shows the maximum electric field in the SiR insulation near the stress cone and high voltage screen tube at different ΔT_2.

TABLE 5. The maximum electric fields in SiR under different temperature differences.

Temperature difference (°C)	10	15	20	25
Maximum electric field of the high voltage screen tube (MV·m^{-1})	3.28	3.15	3.01	2.87
Maximum field strength of the stress cone (MV·m^{-1})	0.22	0.24	0.27	0.31

The results in Table 5 show that the maximum electric field of the screen tube decreased gradually with the increase of ΔT_2, whereas the maximum electric field of the stress cone increased with the increase of ΔT_2. In the case of ΔT_2 at 25 °C, the calculated temperature and maximum electric field near the high voltage screen tube were 50 °C and 2.87 MV/m respectively, whereas the electric field threshold of the SiR at 50 °C was 3.2 MV/m according to the Table 2. Therefore, the amount of space charge accumulation near the high voltage screen tube is insignificant at ΔT_2 of 25 °C.

Fig. 11 shows the electric field distribution on the line segment B-D in Fig.10(b) at different ΔT_2. The results demonstrate that the electric field in the XLPE is reversed at ΔT_2 of 25 °C. Moreover, the electric field in the XLPE is significantly higher than the field in the SiR as the XLPE has evidently low conductivity comparing to the SiR at the same temperature. It is in accordance with the electric field distribution of the insulating materials under the DC voltages.

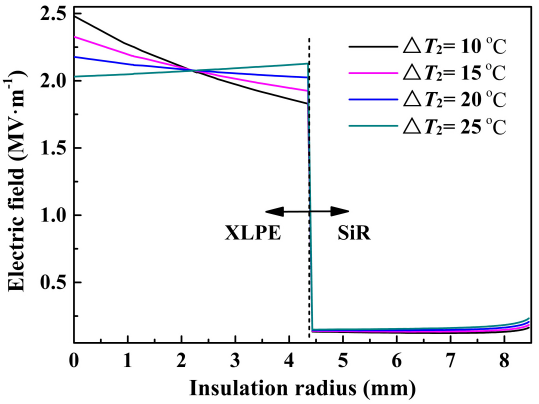

FIGURE 11. The electric field distribution on the line segment B-D at different temperature differences.

The difference of the conductivity in the double-layer materials will generate space charges in the interface. Since the electric field near the stress cone is below the threshold field of the space charge accumulation, Maxwell-Wagner (M-W) theory can be used to estimate the interface space charge density as described in [16] and [20]. The interface space charge can be evaluated by Maxwell's equation. According to Gauss's law, the charge density at the interface between XLPE and SiR is given by

$$\sigma = \varepsilon_2\varepsilon_0 E_2 - \varepsilon_1\varepsilon_0 E_1 \tag{5}$$

where σ is the interface charge density. E_1 and E_2 are perpendicular components of the electric field on the interface of the XLPE and SiR. ε_0 is the vacuum permittivity, ε_1 (=2.3) and ε_2 (=4) are the relative permittivity of the XLPE and SiR, respectively.

Fig. 12 illustrates the interface charge density between XLPE and SiR along the line segment A-C in Fig.10 (b) at different ΔT_2. The results show that the maximum interface charge density appears at A, whereas the interface charge density decreases consistently from A to C. Furthermore, the interface charge density increases with the increase of ΔT_2.

VI. THE FEASIBILITY OF TRANSFORMATION

A. SPACE CHARGE ACCUMULATION

In the case of the electric field below the threshold, the accumulated space charge caused by electrode injection is insignificant. With the increase of the temperature difference

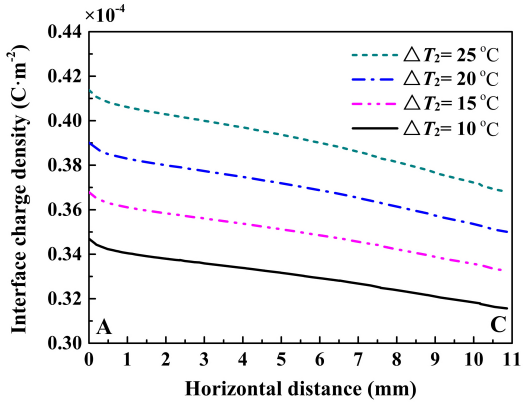

FIGURE 12. The interface charge density along the line segment A-C at different temperature differences.

in the insulation, more bulk charges will naturally accumulate in the insulation. However, the influence of temperature difference on space charge accumulation is not evident [15]. Moreover, the temperature difference in the 10 kV AC XLPE cable insulation is below the data reported in [15], the space charge accumulation in the XLPE insulation is limited. The effect of space charges on the insulation aging can be ignored. The 10 kV AC XLPE cable can be safely operated at DC ±10 kV for a long service time after the AC to DC operation transformation.

The maximum electric field of the cable joint at the high voltage screen tube is higher than the threshold under ΔT_2 of 10 °C. In the case of ΔT_2 at 25 °C, the maximum electric field at the high voltage screen tube is below the threshold, whereas a large temperature difference would naturally introduce a small amount of space charge accumulation in the insulating materials. Space charges could also accumulate at the interface of the XLPE and SiR in the cable joint as described above. The accumulated space charges have potential possibilities to accelerate the aging of the insulating materials in the cable joint.

B. TRANSIENT ELECTRIC FIELD

The 10 kV AC XLPE cable operated under DC voltage might experience different transient voltages, e.g. polarity reversal voltage and impulse voltages. However, there is no polarity reversal process by using voltage source converter (VSC) technology [7], [8] for the DC distribution grid. In the case of impulse voltages, the electric field can be calculated by a superimposition of the steady electric field and transient electric field [19]. The maximum electric field of the cable in DC 10 kV operation is close to the maximum electric field of the cable in AC 10 kV application. Furthermore, the transient electric field in the DC operation is the same as the cable in AC operation due to the permittivity dependent field distribution. The maximum electric field of the cable under DC voltage superimposed with the impulse voltages would be also close to the field of the cable in the AC operation. The 10 kV three-core AC XLPE cable can be operated at ±10 kV with enough safety margin for the transient voltages.

C. MAXIMUM POWER

According to calculations in [21], the ampacity of the three-core 10 kV AC XLPE cable at 70 °C in the DC operation is slightly higher than the ampacity of the cable in the AC operation. Assume the cable running at 65 °C in the DC operation, the ampacity of the cable in the DC operation is equal to the ampacity in the AC operation. The maximum transmission power the cable in AC operation can be obtained by (6), where the power factor $\cos\theta$ is 0.85. According to (7), the maximum transmission power of the cable in the ±10 kV bipolar DC operation is 1.36 times of the power in the AC operation. This indicates that the three-core 10 kV AC XLPE cable running at the ±10 kV bipolar DC is promising for the upgrading of the transmission power in the present distribution grid.

$$P_{AC} = \sqrt{3} \cdot V_{AC} I_{AC} \cos\theta \tag{6}$$

$$P_{DC} = 2 \cdot V_{DC} I_{DC} \tag{7}$$

where P_{AC} and P_{DC} are the AC and DC transmission power respectively. V_{AC} and V_{DC} are the AC and DC voltage respectively. I_{AC} and I_{DC} are the AC and DC ampacity respectively. $\cos\theta$ is the power factor. The AC power and DC power given in this paper are calculated ideally. Some problems in the actual project will have impact on both DC power and AC power. The AC power and DC power need to be analyzed according to specific projects.

VII. CONCLUSION

It has been shown that the electric field threshold of the space charge accumulation for the XLPE and SiR decreases consistently with the increase of the temperature. The threshold of the XLPE is usually higher than the SiR at the same temperature. The threshold of XLPE at 65 °C is 3.1 MV/m, whereas the threshold of SiR at 60 °C is 2.2 MV/m. The DC conductivity of the XLPE and SiR are closely related to the electric field and temperature. The fitted DC conductivity of the XLPE and SiR at different temperatures in the Ohm region is consistent with the measured data. Furthermore, the DC conductivity of the XLPE is lower than the conductivity of the SiR at the same temperature.

It is found that a certain temperature difference is beneficial for balancing the electric field distribution in the insulation. However, the temperature difference between the conductor and insulation screen of 2.5 °C has a higher possibility of the space charge accumulation comparing to the other studied temperature differences. The maximum electric field of the cable operated in DC voltage up to 12.5 kV is lower than the threshold of the space charge accumulation of 3.1 MV/m. The maximum electric field in the cable joint appeared at the high voltage screen tube. Furthermore, the maximum electric field of the cable joint at the high voltage screen tube is higher than the threshold when temperature difference

between the conductor and outer screen is 10 °C, but the maximum electric field at the high voltage screen tube is below the threshold at the temperature difference of 25 °C. The interface charge density increases with the increase of the temperature difference between the conductor and outer screen.

The space charge accumulation in the XLPE insulation is limited in the DC operation, but the space charges could accumulate on the interface between the XLPE and SiR in the cable joint. The maximum transmission power of the cable running at the ±10 kV bipolar DC operation is 1.36 times of the power in the AC operation. Combining to the advantages of the DC distribution grid, it is promising to upgrade the present 10 kV AC distribution grid into ±10 kV DC distribution grid. It must be noted that the results of this paper are indicative, and empirical evidence can be important to derive confidence on these insights.

REFERENCES

[1] L. E. Zubieta, "Are microgrids the future of energy?: DC microgrids from concept to demonstration to deployment," *IEEE Electrific. Mag.*, vol. 4, no. 2, pp. 37–44, Jun. 2016.

[2] K. Mok, M. Wang, S. Tan, and S. Hui, "DC electric springs—A technology for stabilizing DC power distribution systems," *IEEE Trans. Power Electron.*, vol. 32, no. 2, pp. 1088–1105, Feb. 2017.

[3] B. Zhao, Q. Song, J. Li, W. Liu, G. Liu, and Y. Zhao, "High-frequency-link DC transformer based on switched capacitor for medium-voltage DC power distribution application," *IEEE Trans. Power Electron.*, vol. 31, no. 7, pp. 4766–4777, Jul. 2016.

[4] T. B. Wood, D. E. Macpherson, D. Banham-Hall, and S. J. Finney, "Ripple current propagation in bipole HVDC cables and applications to DC grids," *IEEE Trans. Power Del.*, vol. 29, no. 2, pp. 926–933, Apr. 2014.

[5] L. Mackay, R. Guarnotta, A. Dimou, G. Morales-España, L. Ramirez-Elizondo, and P. Bauer, "Optimal power flow for unbalanced bipolar DC distribution grids," *IEEE Access*, vol. 6, no. 1, pp. 5199–5207, Jan. 2018.

[6] D. Kumar, F. Zare, and A. Ghosh, "DC microgrid technology: System architectures, AC grid interfaces, grounding schemes, power quality, communication networks, applications, and standardizations aspects," *IEEE Access*, vol. 5, no. 1, pp. 12230–12256, Jun. 2017.

[7] Y. Liu, X. Cao, and M. Fu, "The upgrading renovation of an existing XLPE cable circuit by conversion of AC line to DC operation," *IEEE Trans. Power Del.*, vol. 32, no. 3, pp. 1321–1328, Jun. 2017.

[8] J. Yu, K. Smith, M. Urizarbarrena, N. Macleod, R. Bryans, and A. Moon, "The upgrading renovation of an existing XLPE cable circuit by conversion of AC line to DC operation," in *Proc. IET Int. Conf. AC DC Power Transmiss.*, Manchester, U.K., 2017, pp. 1–6.

[9] G. C. Montanari, G. Mazzanti, F. Palmieri, A. Motori, G. Perego, and S. Serra, "Space-charge trapping and conduction in LDPE, HDPE and XLPE," *J. Phys. D, Appl. Phys.*, vol. 34, no. 18, pp. 2902–2911, Sep. 2001.

[10] D. Fabiani *et al.*, "Polymeric HVDC cable design and space charge accumulation. Part 1: Insulation/semicon interface," *IEEE Elect. Insul. Mag.*, vol. 23, no. 6, pp. 11–19, Nov. 2007.

[11] G. C. Montanari and P. H. F. Morshuis, "Space charge phenomenology in polymeric insulating materials," *IEEE Trans. Dielectr. Electr. Insul.*, vol. 12, no. 4, pp. 754–767, Aug. 2005.

[12] L. A. Dissado, C. Laurent, G. C. Montanari, and P. H. F. Morshuis, "Demonstrating a threshold for trapped space charge accumulation in solid dielectrics under DC field," *IEEE Trans. Dielectr. Electr. Insul.*, vol. 12, no. 3, pp. 612–620, Jun. 2005.

[13] R. Bodega, G. C. Montanari, and P. H. F. Morshuis, "Conduction current measurements on XLPE and EPR insulation," in *Proc. 17th Annu. Meeting IEEE Lasers Electro-Opt. Soc.*, Boulder, CO, USA, Oct. 2004, pp. 101–105.

[14] G. C. Montanari, "The electrical degradation threshold of polyethylene investigated by space charge and conduction current measurements," *IEEE Trans. Dielectr. Electr. Insul.*, vol. 7, no. 3, pp. 309–315, Jun. 2000.

[15] B. X. Du, C. Han, Z. Li, and J. Li, "Effect of graphene oxide particles on space charge accumulation in LDPE/GO nanocomposites," *IEEE Trans. Dielectr. Electr. Insul.*, vol. 25, no. 4, pp. 1479–1486, Aug. 2018.

[16] B. X. Du, Z. L. Li, and Z. R. Yang, "Field-dependent conductivity and space charge behavior of silicone rubber/SiC composites," *IEEE Trans. Dielectr. Electr. Insul.*, vol. 23, no. 5, pp. 3108–3116, Oct. 2016.

[17] D. Fabiani *et al.*, "Feature article—HVDC cable design and space charge accumulation. Part 3: Effect of temperature gradient," *IEEE Electr. Insul. Mag.*, vol. 24, no. 2, pp. 5–14, Apr. 2008.

[18] T. T. N. Vu, G. Teyssedre, B. Vissouvanadin, S. L. Roy, and C. Laurent, "Correlating conductivity and space charge measurements in multi-dielectrics under various electrical and thermal stresses," *IEEE Trans. Dielectr. Electr. Insul.*, vol. 22, no. 1, pp. 117–127, Feb. 2015.

[19] Y. Liu, S. Zhang, X. Cao, C. Zhang, and W. Li, "Simulation of electric field distribution in the XLPE insulation of a 320 kV DC cable under steady and time-varying states," *IEEE Trans. Dielectr. Electr. Insul.*, vol. 25, no. 3, pp. 954–964, Jun. 2018.

[20] S. Delpino, D. Fabiani, G. C. Montanari, and C. Laurent, "Feature article—Polymeric HVDC cable design and space charge accumulation. Part 2: Insulation interfaces," *IEEE Electr. Insul. Mag.*, vol. 24, no. 1, pp. 14–24, Feb. 2008.

[21] J. Yu *et al.*, "Numerical analysis of thermo-electric field for 10 kV AC XLPE cable in DC operation," in *Proc. 12th Int. Conf. Properties Appl. Dielectr. Mater.*, Xi'an, China, 2018, pp. 629–632.

XIANGRONG CHEN (S'08–M'11) was born in Hunan , China, in 1982. He received the M.S. and Ph.D. degrees in electrical engineering from Xi'an Jiaotong University, China, in 2008 and 2011, respectively. He was a Postdoctoral, in 2011, was an Assistant Professor, from 2012 to 2016, and was an Associate Professor, in 2016, in high voltage engineering with the Department of Manufacturing and Materials Technology, Chalmers University of Technology, Gothenburg, Sweden. Since 2017, he has been a One-Hundred Talents Researcher/Professor and has been the Head of the High Voltage Technology, College of Electrical Engineering, Zhejiang University, China. His research interests include HVDC power transmission, ac/dc cable technology, advanced dielectric materials, advanced measuring and sensing technology, and high voltage new technology.

JINGZHE YU (S'18) was born in Hebei, China, in 1991. He received the B.S. degree in electrical engineering from Guangxi University, China, in 2015. He is currently pursuing the Ph.D. degree with the College of Electrical Engineering, Zhejiang University. His main research interests include HVDC power transmission, cable technology, numerical simulation, dielectric properties, and space charge of polymer insulating materials for XLPE cables.

LINWEI YU was born in Guangxi, China, in 1995. He received the bachelor's degree from Zhejiang University, China, in 2017, where he is currently pursuing the master's degree with the College of Electrical Engineering. His main interests include high voltage insulation testing, space charge measurements, and the application of voltage stabilizers in polyethylene.

HAO ZHOU was born in Zhejiang, China, in 1963. He received the M.S. and Ph.D. degrees in electrical engineering from Zhejiang University, Hangzhou, China, in 1989 and 2004, respectively. Since 2007, he has been a Professor in high voltage engineering with the Department of Electrical Engineering, Zhejiang University. His research interests include ultra-high voltage ac/dc power transmission, overvoltage, and insulation coordination for HVAC/HVDC power system.